Self-Energy on the Low- to High-Energy Electronic Structure of Correlated Metal $SrVO_3$

S. Aizaki,[1] T. Yoshida,[1] K. Yoshimatsu,[2] M. Takizawa,[1,*] M. Minohara,[2] S. Ideta,[1] A. Fujimori,[1] K. Gupta,[3] P. Mahadevan,[3] K. Horiba,[2,5] H. Kumigashira,[4,5] and M. Oshima[2,5]

[1]*Department of Physics, The University of Tokyo, Tokyo 113-0033, Japan*
[2]*Department of Applied Chemistry, The University of Tokyo, Tokyo 113-0033, Japan*
[3]*S. N. Bose National Centre for Basic Sciences, Kolkata 700-098, India*
[4]*KEK, Photon Factory, Tsukuba, Ibaraki 305-0801, Japan*
[5]*JST-CREST, Tokyo 102-0075, Japan*

(Received 20 December 2011; published 31 July 2012)

The correlated electronic structure of $SrVO_3$ has been investigated by angle-resolved photoemission spectroscopy using *in situ* prepared thin films. Pronounced features of band renormalization have been observed: a sharp kink ~60 meV below the Fermi level (E_F) and a broad so-called "high-energy kink" ~0.3 eV below E_F as in the high-T_c cuprates, although $SrVO_3$ does not show magnetic fluctuations. We have deduced the self-energy in a wide energy range by applying the Kramers-Kronig relation to the observed spectra. The obtained self-energy clearly shows a large energy scale of ~0.7 eV, which is attributed to electron-electron interaction and gives rise to the ~0.3 eV kink in the band dispersion as well as the incoherent peak ~1.5 eV below E_F. The present analysis enables us to obtain a consistent picture for both the incoherent spectra and the band renormalization.

DOI: 10.1103/PhysRevLett.109.056401 PACS numbers: 71.18.+y, 71.20.−b, 71.27.+a, 71.30.+h

The effect of many-body interaction on the electronic structure, such as electron correlation or electron-phonon interactions, is an important concept for understanding the physical properties of materials and, hence, is one of the most fundamental issues in condensed matter physics. In a correlated electron system, coupling of single-particle excitations with collective excitations such as phonons leads to a pronounced energy-dependent band renormalization, a so-called kink, in the band dispersion. In the studies of high-T_c cuprate superconductors by angle-resolved photoemission spectroscopy (ARPES), a kink has been observed around ~60 meV below E_F [1] in the nodal region of the Fermi surface, where no superconducting gap opens. Moreover, a high-energy kink has also been observed around 0.3–0.4 eV below E_F [2,3], and its origin has been debated. Electron-phonon interaction [1], antiferromagnetic fluctuations, and/or the magnetic resonance mode [4] have been proposed as possible origins of the low-energy kink. As for the high-energy kink [2], short-range Coulomb interaction [3], a disintegration of an electron into a spinon and holon high-energy spin fluctuations [5], loop-current fluctuations [6], and electron correlation [7] have been proposed as possible candidates. In order to clarify the origin of the high-energy kink, studies of kinks in transition-metal oxides other than the cuprates will give useful information.

$SrVO_3$ (SVO) is one of the perovskite-type light transition-metal oxides (TMOs) and is a prototypical Mott-Hubbard-type system with the d^1 electronic configuration. Therefore, SVO is an ideal system to study the fundamental physics of electron correlation and has been extensively studied by photoemission spectroscopy measurements [8–18]. Also, the electronic structure of this system has been studied by a dynamical mean-field theory (DMFT) calculation [16,17], because the system is ideal for the realistic modeling of correlated materials. In a DMFT calculation by Nekrasov *et al.* [17], SVO has foreseen the existence of a high-energy kink caused by a general property of electron-electron interaction and, hence, a general feature of the electron self-energy of correlated metals. In an ARPES study of bulk SVO [18], the mass enhancement factor m^*/m_b of the V $3d$ band was estimated to be ~2, consistent with the bulk thermodynamic properties [10]. A subsequent ARPES study of bulk SVO and $CaVO_3$ (CVO) revealed that the bandwidth indeed decreased by ~20% in going from SVO to CVO [19]. Recently, more detailed ARPES measurements have been achieved by the growth of high-quality films having atomically flat surfaces using the pulsed laser deposition (PLD) technique. Takizawa *et al.* [20] and Yoshimatsu *et al.* [21] fabricated SVO thin films using the PLD and studied its detailed electronic structure by *in situ* ARPES measurements. Clear band dispersions were observed not only in the coherent quasiparticle (QP) part but also in the incoherent part, consistent with the DMFT calculation [17].

In the present work, we have investigated the existence or absence of the low- and high-energy kinks in SVO with improved sample quality and instrumental resolution. A pronounced effect of energy-dependent band renormalization, namely a kink, has been observed at the binding energy of ~60 meV and a high-energy kink at ~0.3 eV. Since SVO is a Pauli-paramagnetic metal without any signature of magnetic fluctuations, the presence of the kinks will give us a clue to understanding the nature of the interaction which gives rise to the kinks. Furthermore,

we deduced the self-energy $\Sigma(\mathbf{k}, \omega)$ in a wide energy range through Kramers-Kronig analysis [7,22].

In situ photoemission measurements in the valence-band and core-level regions were performed at beam lines 28A and 2C of the Photon Factory (PF) using a Scienta SES-2002 and SES-100 electron analyzer, respectively. For the measurement at beam line 28A, photon energies $h\nu = 50$ to 106 eV were used with the total energy resolutions of 20–30 meV and the momentum resolution of 0.3 degree. The present energy resolution is high enough to detect the kink ~60 meV near the E_F. Epitaxial thin films of SVO were grown on single-crystal, Nb-doped $SrTiO_3$ (001) substrates by the PLD method. The substrates were annealed at 1050 °C under an oxygen pressure of $\sim 1 \times 10^{-6}$ Torr to obtain an atomically flat TiO_2-terminated surface. SVO thin films were deposited on the substrates at 900 °C under a high vacuum of $\sim 10^{-8}$ Torr. The chemical composition was checked by core-level photoemission spectra and the surface morphology by *ex situ* atomic force microscopy, showing atomically flat step-and-terrace structures. ARPES measurements were performed in an ultrahigh vacuum better than 1×10^{-10} Torr below 20 K. In-plane electron momenta k_x and k_y are expressed in units of π/a, where $a = 3.905$ Å is the in-plane lattice constant of the SVO thin film, identical to that of the $SrTiO_3$ substrate. Electron momentum in the out-of-plane k_z direction is expressed in units of π/c, where $c = 3.82$ Å is the out-of-plane lattice constant of the SVO thin film determined by x-ray diffraction reciprocal space mapping.

In SVO, each of the d_{xy}, d_{yz}, and d_{zx} orbitals forms a nearly two-dimensional band. Consequently, the Fermi surfaces (FSs) consist of three cylinders penetrating perpendicularly to each other. Figure 1(a) shows ARPES spectra near E_F along the cuts in the Fermi surface mapping of Fig. 1(b). There are two main features near E_F: the coherent part (the sharp QP peak within ~0.5 eV of E_F) and the broad incoherent part (often regarded as the remnant of the lower Hubbard band centered ~1.5 eV below E_F). As reported before [18,20], the coherent part shows a clear band dispersion.

In order to examine the three-dimensional electronic structure, we obtained the E_F intensity map in k_x-k_z space by changing the photon energy as shown in Fig. 1(c). Here, the k_z values have been obtained by assuming the inner potential of $V_0 = 18$ eV and the work function of $\phi = 4.5$ eV. The assumed parameters are nearly the same as the ARPES results of bulk SVO and CVO [19] and reasonably account for the periodicity of the FSs along the k_z direction shown in Fig. 1(c). The intensity distribution indicates that the d_{xy} FS is nearly a straight cylinder along the k_z direction and is therefore two dimensional. On the other hand, the d_{zx} and d_{yz} FSs are not clearly observed due to matrix-element effect and k_z broadening.

We shall investigate correlation effects in the QP spectra by close examination of the nearly two-dimensional d_{xy} band. Image plots of the d_{xy} band in E-k_x space are shown in Fig. 2(a). Here, QP band dispersions are determined by the peak positions of the momentum distribution curves (MDCs) and the second derivative of the energy distribution curves (EDCs). Note that the spectral intensity at the bottom of the dispersion is suppressed due to matrix-element effect. Hence, the dispersion near the band bottom is well represented by EDC peaks, while the MDC peaks well represent that near E_F. By smoothly connecting the MDC peak dispersion and the EDC dispersion in an intermediate energy region of ~0.25 eV, one can obtain a reasonable picture of the d_{xy} band dispersion in the entire energy range.

In order to deduce the real part of the self-energy $\Sigma(\mathbf{k}, \omega)$, we use the noninteracting band dispersion calculated within the local-density approximation (LDA) (red curve) and take the difference between the band dispersions and the LDA band as shown in Fig. 2(b). Because the observed k_F values are a few percent larger than those in the LDA band, the LDA band has been shifted downward to make $\mathrm{Re}\Sigma(0) = 0$. The nearly identical $\Sigma(\mathbf{k}, \omega)$ for cuts A and B indicates that the self-energy $\sum$ is nearly $\mathbf{k}$ independent at least within the studied momenta. In the deduced $\mathrm{Re}\Sigma(\mathbf{k}, \omega)$, a kink is seen around 60 meV below E_F and shall be referred to as the "low-energy kink," very

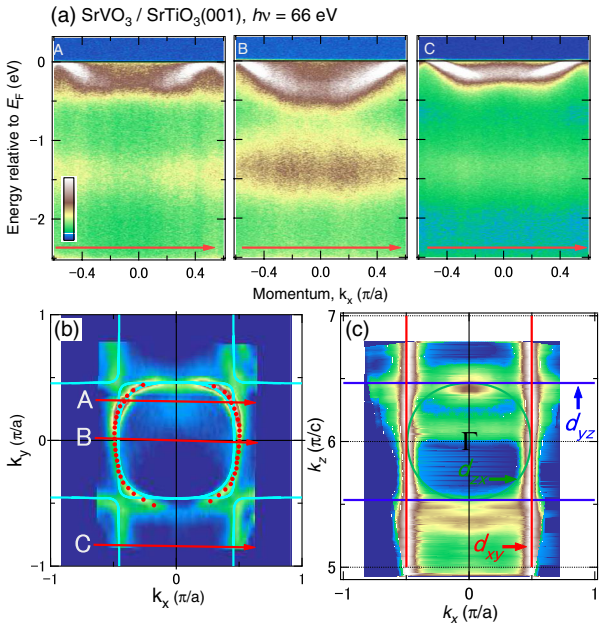

FIG. 1 (color online). ARPES spectra of $SrVO_3$. (a) Intensity plots in E-k space for cuts A, B, and C shown in panel (b) taken at the photon energy of 66 eV with linear polarization. (b) Intensity map at E_F revealing the nearly circular cross section of the d_{xy} Fermi surface. Dots show the k_F points determined by MDC peak positions at E_F. Solid curves are the FSs given by the LDA band-structure calculation. (c) Spectral weight mapping in k_x-k_z space obtained using photon energies $h\nu = 50$–106 eV. Tight-binding bands fitted to the Fermi surfaces are shown by circular and straight lines.

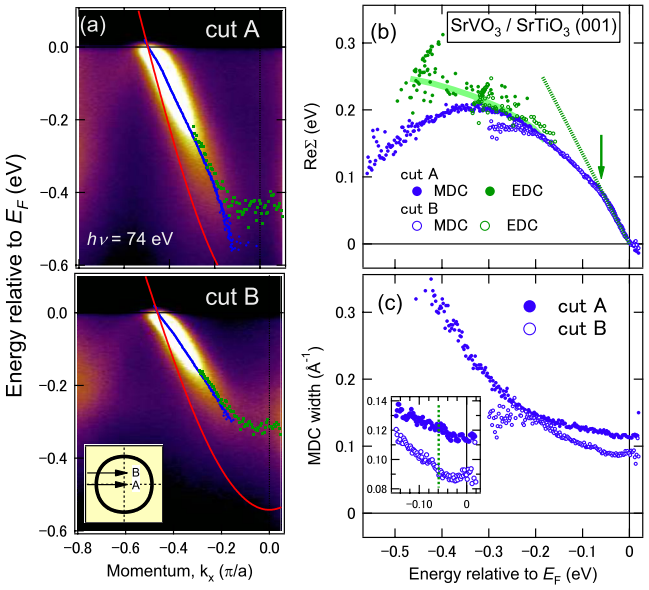

FIG. 2 (color online). Band dispersions and self-energies in the vicinity of the Fermi level. (a) Intensity plots for cuts shown in inset. QP band dispersions are determined by the MDC peak positions (blue dots), which are correct near E_F, and the second derivative of EDCs (green dots), which are correct near the band bottom. The noninteracting band given by the LDA band-structure calculation is shown by red curves. (b) Real part of the self-energy $\mathrm{Re}\Sigma(\omega)$. Here, we have obtained $\mathrm{Re}\Sigma(\omega)$ as the difference between the band determined by the experimental band dispersion and the LDA energy band dispersion. The position of the kink at ~60 meV is shown by an arrow. (c) Energy dependence of the MDC width, which is proportional to the imaginary part of the self-energy $\mathrm{Im}\Sigma(\omega)$. Inset is enlarged plots near E_F, which also indicates the kink at ~60 meV.

similar to those observed in the high-T_c cuprate superconductors. As shown in Fig. 2(c), the signature of the kink is also seen in the MDC width, which is proportional to $\mathrm{Im}\Sigma(\omega)$. Lanzara *et al.* related the kink in the high-T_c cuprates with the oxygen half-breathing phonon mode of ~60 meV [1]. In Raman scattering measurements of the perovskite-type compounds, Jahn-Teller phonons and oxygen breathing phonons are always observed in the region of 60–90 meV [23,24]. Also, since SVO, unlike the cuprates, does not have low-energy spin fluctuations, the kink observed in the present study is likely due to a coupling of electrons with these phonon modes characteristic to the perovskite oxides.

The $\mathrm{Re}\Sigma(\omega)$ thus deduced shows not only the low-energy kink (~ -60 meV) but also a weak, broad kink at -0.3–0.4 eV, again similar to the high-energy kink of the high-T_c cuprates. Here, it should be noted that if MDC peaks are used to deduce $\mathrm{Re}\Sigma(\omega)$ in the entire energy range, the high-energy kink feature is overemphasized compared to the actual high-energy kink. Therefore, the correct deduction of the experimental band dispersion using both MDC and EDC peaks is necessary to study the high-energy kink phenomena.

The energy range of $\mathrm{Re}\Sigma(\mathbf{k}, \omega)$ and $\mathrm{Im}\Sigma(\mathbf{k}, \omega)$ studied by the above method is limited to ~0.5 eV below E_F, the energy range of the coherent part, while the behavior of the self-energy over a wider energy range is necessary to understand the role of electron correlation or the incoherent part, too. Therefore, we deduce the self-energy in a wider energy range using the Kramers-Kronig (KK) relation as follows. By performing the KK transformation of the spectral function $A(\mathbf{k}, \omega) = -\mathrm{Im}G(\mathbf{k}, \omega)/\pi$, one can obtain $\mathrm{Re}G(\mathbf{k}, \omega)$ and, consequently, $G(\mathbf{k}, \omega) = 1/(\omega - \epsilon_k - \Sigma(\mathbf{k}, \omega))$ and, hence, $\epsilon_k + \Sigma(\mathbf{k}, \omega)$. However, the ARPES intensity only gives $A(\mathbf{k}, \omega)$ below E_F. Therefore, in the present analysis, several assumptions have been made to deduce the self-energy. First, we assume electron-hole symmetry for the self-energy, which can be justified near E_F: $\mathrm{Re}\Sigma(\mathbf{k}, \omega) = -\mathrm{Re}\Sigma(\mathbf{k}, -\omega)$ and $\mathrm{Im}\Sigma(\mathbf{k}, \omega) = \mathrm{Im}\Sigma(\mathbf{k}, -\omega)$. To obtain the self-energy self-consistently under this assumption, we use the experimental ARPES intensity $I(\mathbf{k}, \omega)$ and construct the initial function for $A(\mathbf{k}, \omega)$ as $A(\mathbf{k}, \omega) = I(\mathbf{k}, \omega)(k < k_F)$, $A(\mathbf{k}, \omega) = I(\mathbf{k}, \omega) + I(\mathbf{k}, -\omega)(k = k_F)$. Here, $A(\mathbf{k}, \omega)$ $(k < k_F)$ for $\omega > 0$ is assumed to be much smaller than those for $\omega < 0$ because the band dispersion ϵ_k is below the E_F. By KK transforming $A(\mathbf{k}, \omega)$, $\mathrm{Re}\Sigma(\mathbf{k}, \omega)$ and $\mathrm{Im}\Sigma(\mathbf{k}, \omega)$ are obtained. In order to fulfill the electron-hole symmetry, the $\Sigma(\mathbf{k}, \omega)$ for $\omega > 0$ is set equal to the complex conjugate of $-\Sigma(\mathbf{k}, \omega)$ for $\omega < 0$. Then, $A(\mathbf{k}, \omega)$ can be renewed by using the new $\Sigma(\mathbf{k}, \omega)$. This process is repeated iteratively until $A(\mathbf{k}, \omega)$ and $\Sigma(\mathbf{k}, \omega)$ are converged. Note that the converged $A(\mathbf{k}, \omega)$ shows nearly identical spectral line shape, such as the energy and width of the peak, to $I(\mathbf{k}, \omega)$ for $\omega < 0$, indicating that the assumptions described above were reasonably realistic and the resulting self-energy is a good approximation for the true self-energy in the wide energy range of a few eV.

The input $A(\mathbf{k}, \omega)$ is taken from cut B in Fig. 1, and the integrated background and the tail of the O $2p$ band have been subtracted. Thus obtained $A(\mathbf{k}, \omega)$ for $k \leq k_F$ is shown in Fig. 3(a). Panels (b) and (c) show $\mathrm{Re}\Sigma$ and $\mathrm{Im}\Sigma$, respectively, derived from $A(\mathbf{k}, \omega)$ in panel (a). The deduced $\Sigma(\mathbf{k}, \omega)$s for each momentum show similar line shapes, but there is a weak momentum dependence. Particularly, the absolute value of the $\Sigma(\mathbf{k}, \omega)$ for $k = k_F$ is larger than those for other momenta. Assuming that the momentum dependence of Σ is symmetric with respect to k_F, the average of the self-energy over the Brillouin zone has been obtained as shown in Fig. 3(d). The low energy part of the iteratively deduced self-energy qualitatively agrees with the self-energy deduced from the band dispersion as shown in the inset of Fig. 3(d).

The noninteracting band dispersion ϵ_k is related to $G(\mathbf{k}, \omega)$ through $\mathrm{Re}[-1/G(\mathbf{k}, 0)] = \epsilon_k$. Figure 3(f) demonstrates good agreement between the experimentally deduced $\mathrm{Re}[-1/G(\mathbf{k}, 0)]$ and the band dispersion predicted by the band-structure calculation [25]. Interestingly, this

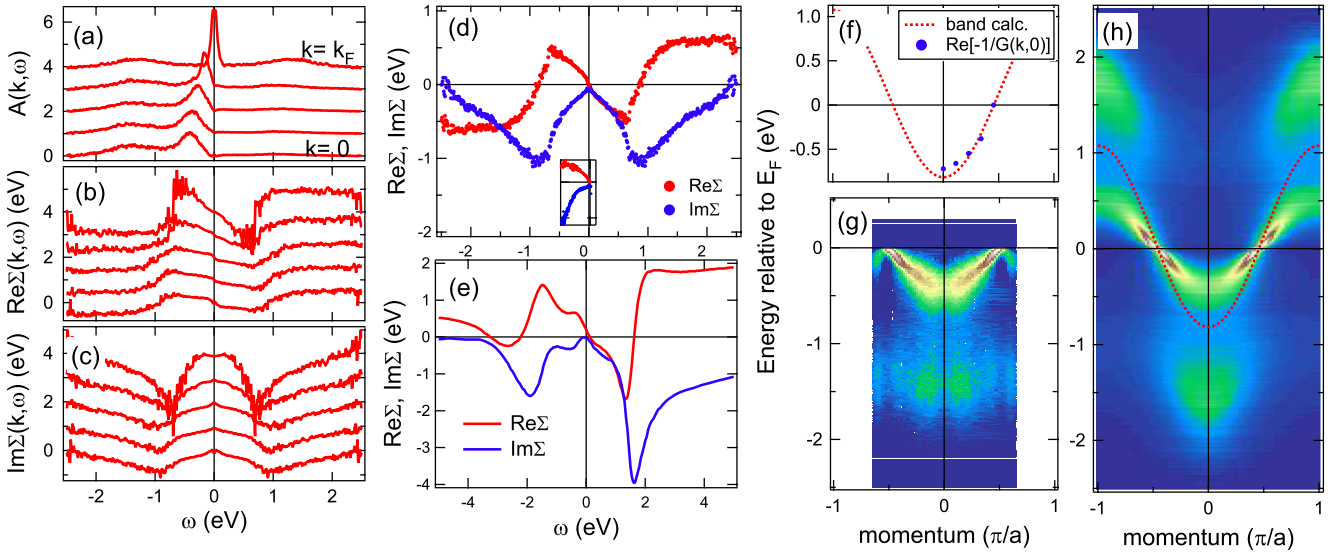

FIG. 3 (color online). Self-energy iteratively deduced from the measured ARPES spectra using the Kramers-Kronig transformation. (a): $A(k, \omega)$ calculated using the self-energy in panels (b) and (c). (b) and (c): ReΣ and ImΣ plotted as a function of energy for various momenta. (d) Average of ReΣ and ImΣ over the momentum. For comparison, the ReΣ and ImΣ (shifted by 0.3 eV) obtained in Fig. 2 are shown in inset. (e) Self-energy predicted by the LDA + DMFT calculation of Ref. [26]. (f) Comparison of Re$[-1/G(k, 0)](= \epsilon_k)$ obtained from the experimental data with the LDA band dispersion [25]. (g) Intensity plot of the ARPES data. (h) Simulation of the spectral function $A(k, \omega) = -\mathrm{Im}\, G(k, \omega)/\pi$ using the momentum-averaged self-energy in panel (d) and the LDA energy band.

analysis demonstrates that the noninteracting band can be extracted from experimental data which are influenced by electron correlation. One can, therefore, conclude that it is self-consistent to use the band-structure calculation for ϵ_k in the present analysis. In Figs. 3(g) and 3(h), we compare the ARPES intensity plot and the simulated intensity distribution $A(\mathbf{k}, \omega)$ in E-k space. Here, we have calculated $A(\mathbf{k}, \omega)$ using the momentum-averaged $\Sigma(\omega)$ [Fig. 3(d)] and the result of the band-structure calculation ϵ_k [25]. The QP dispersions and the incoherent part shown in Fig. 3(g) are successfully reproduced by the simulation as shown in Fig. 3(h), indicating the self-consistency of the deduced self-energy.

The ReΣ and ImΣ iteratively deduced from the experiment exhibit the characteristic behaviors predicted by the DMFT study of the Hubbard model [7]. For example, ReΣ shows a maximum at $\omega \sim -0.7$ eV, where the EDC shows an intensity minimum. In Figs. 3(d) and 3(e), we compare the experimental self-energy and the self-energy calculated for SVO by the LDA + DMFT method [26]. The experimental self-energy shows remarkably similar behavior to that of the LDA + DMFT, although both the vertical and horizontal axes are different by a factor of two [see panels (d) and (e)].

As for the high-energy kink, while the theory predicts a pronounced feature ~0.3 eV below E_F, the experimental kink in the same energy region is less pronounced. The kink which we observed at ~60 meV (Fig. 2) is not reproduced by the calculation because electron-phonon coupling is not included in the theoretical model. As for the incoherent part, while the peak energy of the LDA + DMFT calculation is ~2.1 eV below E_F [26], that in the present result is ~1.5 eV below it, suggesting that electron correlation is overestimated in the calculation. On the other hand, both the QP band in the experiment and that from the calculation show a renormalization factor of ~2 relative to the LDA band dispersion. This is because the slope of Re$\Sigma(\omega)$ near E_F is nearly the same between the experimental and the theoretical self-energies as shown in Figs. 3(d) and 3(e). Therefore, in order to achieve a consistent picture of the correlated electronic structure, further development of the theoretical approaches and the extension of the experimental approach to other correlated systems have to be made in future studies.

In conclusion, we have performed a detailed ARPES study of *in situ-prepared* SVO thin films and revealed self-energy effects on the QPs as well as the incoherent structure. A low-energy kink was observed at the binding energy ~60 meV as in the case of the high-T_c cuprate superconductors. Since low-energy spin fluctuations are not identified in SVO, the kink observed in the present study is likely due to a coupling with the phonon modes characteristic to the perovskite oxides [23,24]. We have obtained the self-energy in a wide energy range by applying the KK relation to the experimental spectral function. The self-energy shows a large-energy scale of ~0.7 eV reflecting electron-electron interaction and giving rise to the broad high-energy kink ~0.3 eV below E_F as well as the incoherent peak ~1.5 eV below E_F. The present result provides a self-consistent procedure to experimentally

deduce the self-energy in correlated electron systems, and this procedure would be useful for future studies of electron correlation effects.

The authors would like to thank A. Georges and S. Biermann for discussion and K. Ono, J. Adachi, and M. Kubota for their support in the experiment at KEK-PF. This work was supported by a Grant-in-Aid for Scientific Research (S)(22224005), a Grant-in-Aid for Young Scientist (B) (22740221), a Grant-in-Aid for Scientific Research on Innovative Area "Materials Design through Computics: Complex Correlation and Non-Equilibrium Dynamics," and an Indo-Japan Joint Research Project "Nobel Magnetic Oxide Nano-Materials Investigated by Spectroscopy and ab-initio Theories" from JSPS. The work in Kolkata was supported by DST, India. The experiments were done under the approval of the Photon Factory Program Advisory Committee (Proposals No. 2007G597 and No. 2008S2-003) at the Institute of Material Structure Science, KEK.

*Present address: Research Organization of Science and Engineering, Ritsumeikan University, 1-1-1 Noji-Higashi, Kusatsu, Shiga 525-8577, Japan.

[1] A. Lanzara, P. V. Bogdanov, X. J. Zhou, S. A. Kellar, D. L. Feng, E. D. Lu, T. Yoshida, H. Eisaki, A. Fujimori, K. Kishio, J.-I. Shimoyama, T. Noda, S. Uchida, Z. Hussain, and Z.-X. Shen, Nature (London) **412**, 510 (2001).

[2] J. Graf, G.-H. Gweon, K. McElroy, S. Y. Zhou, C. Jozwiak, E. Rotenberg, A. Bill, T. Sasagawa, H. Eisaki, S. Uchida, H. Takagi, D.-H. Lee, and A. Lanzara, Phys. Rev. Lett. **98**, 067004 (2007).

[3] W. Meevasana *et al.*, Phys. Rev. B **75**, 174506 (2007).

[4] P. D. Johnson, T. Valla, A. V. Fedorov, Z. Yusof, B. O. Wells, Q. Li, A. R. Moodenbaugh, G. D. Gu, N. Koshizuka, C. Kendziora, S. Jian, and D. G. Hinks, Phys. Rev. Lett. **87**, 177007 (2001).

[5] A. Macridin, M. Jarrell, T. Maier, and D. J. Scalapino, Phys. Rev. Lett. **99**, 237001 (2007).

[6] L. Zhu, V. Aji, A. Shekhter, and C. M. Varma, Phys. Rev. Lett. **100**, 057001 (2008).

[7] K. Byczuk, M. Kollar, K. Held, Y.-F. Yang, I. A. Nekrasov, T. Pruschke, and D. Vollhardt, Nature Phys. **3**, 168 (2007).

[8] M. Imada, A. Fujimori, and Y. Tokura, Rev. Mod. Phys. **70**, 1039 (1998).

[9] A. Fujimori, I. Hase, H. Namatame, Y. Fujishima, Y. Tokura, H. Eisaki, S. Uchida, K. Takegahara, and F. M. F. de Groot, Phys. Rev. Lett. **69**, 1796 (1992).

[10] I. H. Inoue, O. Goto, H. Makino, N. E. Hussey, and M. Ishikawa, Phys. Rev. B **58**, 4372 (1998).

[11] I. H. Inoue, I. Hase, Y. Aiura, A. Fujimori, Y. Haruyama, T. Maruyama, and Y. Nishihara, Phys. Rev. Lett. **74**, 2539 (1995).

[12] A. Sekiyama, H. Fujiwara, S. Imada, S. Suga, H. Eisaki, S. I. Uchida, K. Takegahara, H. Harima, Y. Saitoh, I. A. Nekrasov, G. Keller, D. E. Kondakov, A. V. Kozhevnikov, T. Pruschke, K. Held, D. Vollhardt, and V. I. Anisimov, Phys. Rev. Lett. **93**, 156402 (2004).

[13] R. Eguchi, T. Kiss, S. Tsuda, T. Shimojima, T. Mizokami, T. Yokoya, A. Chainani, S. Shin, I. H. Inoue, T. Togashi, S. Watanabe, C. Q. Zhang, C. T. Chen, M. Arita, K. Shimada, H. Namatame, and M. Taniguchi, Phys. Rev. Lett. **96**, 076402 (2006).

[14] K. Maiti, D. D. Sarma, M. J. Rozenberg, I. H. Inoue, H. Makino, O. Goto, M. Pedio, and R. Cimino, Europhys. Lett. **55**, 246 (2001).

[15] H. Wadati, T. Yoshida, A. Chikamatsu, H. Kumigashira, M. Oshima, H. Eisaki, Z.-X. Shen, T. Mizokawa, and A. Fujimori, Phase Transit. **79**, 617 (2006).

[16] A. Georges, G. Kotliar, W. Krauth, and M. J. Rozenberg, Rev. Mod. Phys. **68**, 13 (1996).

[17] I. A. Nekrasov, G. Keller, D. E. Kondakov, A. V. Kozhevnikov, T. Pruschke, K. Held, D. Vollhardt, and V. I. Anisimov, Phys. Rev. B **72**, 155106 (2005).

[18] T. Yoshida, K. Tanaka, H. Yagi, A. Ino, H. Eisaki, A. Fujimori, and Z.-X. Shen, Phys. Rev. Lett. **95**, 146404 (2005).

[19] T. Yoshida, M. Hashimoto, T. Takizawa, A. Fujimori, M. Kubota, K. Ono, and H. Eisaki, Phys. Rev. B **82**, 085119 (2010).

[20] M. Takizawa, M. Minohara, H. Kumigashira, D. Toyota, M. Oshima, H. Wadati, T. Yoshida, A. Fujimori, M. Lippmaa, M. Kawasaki, H. Koinuma, G. Sordi, and M. Rozenberg, Phys. Rev. B **80**, 235104 (2009).

[21] K. Yoshimatsu, K. Horiba, H. Kumigashira, T. Yoshida, A. Fujimori, and M. Oshima, Science **333**, 319 (2011).

[22] M. R. Norman, H. Ding, H. Fretwell, M. Randeria, and J. C. Campuzano, Phys. Rev. B **60**, 7585 (1999).

[23] S. Sugai and K. Hirota, Phys. Rev. B **73**, 020409 (2006).

[24] E. Siranidi, D. Lampakis, D. Palles, E. Liarokapis, C. Colin, and T. T. M. Palstra, J. Supercond. Nov. Magn. **22**, 185 (2009).

[25] E. Pavarini, S. Biermann, A. Poteryaev, A. I. Lichtenstein, A. Georges, and O. K. Andersen, Phys. Rev. Lett. **92**, 176403 (2004).

[26] I. A. Nekrasov, K. Held, G. Keller, D. E. Kondakov, T. Pruschke, M. Kollar, O. K. Andersen, V. I. Anisimov, and D. Vollhardt, Phys. Rev. B **73**, 155112 (2006).